Program Digest, 2019 IEEE International Ultrasonics Symposium (IUS)
Glasgow, Scotland, October 6-9, 2019

Effects of Acoustic Nonlinearities on the Estimation of Attenuation from Ultrasonic Backscatter

Andres Coila, *Student Member, IEEE,* and Michael Oelze, *Member, IEEE*

Abstract— **The attenuation coefficient (AC) has demonstrated the ability to classify tissue state. Linear acoustic propagation is assumed when estimating the AC using spectral-based methods from the ultrasonic backscatter. However, the effects of acoustic nonlinearities can distort the backscattered power spectra versus depth. The distortion of the power spectra could result in a bias in the estimation of the AC. The goal of the study was to quantify the effects of nonlinear distortion on the estimation of AC from ultrasonic backscatter using spectral methods. We computed the AC from backscattered signals using the spectral log difference method and a reference phantom to account for diffraction effects. Computational simulations and experiments in phantoms were performed. In the experiments, three tissue-mimicking phantoms, named A, B and C having estimated AC values of 0.60, 0.90, and 0.20 dB/cm/MHz, respectively, and $B/A \approx 6.6$ for each phantom were scanned using a single-element focused transducer (f/2) having a 0.5" diameter and 5-MHz center frequency. The phantoms were scanned using six excitation levels from a high-power (HP) pulsing apparatus (RAM-5000, Ritec, USA). The AC was estimated from phantom A using either phantom B (high attenuation) or phantom C (low attenuation) as the reference. The AC was estimated at each excitation level over the analysis bandwidth (-6-dB criterion) to determine the effects of acoustic nonlinearity on estimation of AC. The presence of nonlinear distortion can be quantified through the Gol'dberg number, which is inversely proportional to the product of the nonlinearity coefficient and attenuation. We hypothesized that because the B/A values were approximately the same for each phantom, the effects of nonlinear distortion would be more pronounced when using phantom C, which had much lower attenuation. Specifically, increased excess attenuation due to transfer of energy from the fundamental to the harmonics would be observed more in phantom C. The AC estimate increased from 0.57 to 0.67 dB/cm/MHz as the excitation levels increased from level one to six when using phantom B as a reference. In contrast, when using phantom C as reference, the estimated AC slope of phantom A decreased from 0.57 to 0.43 dB/cm/MHz as the excitation levels increased from level one to six. Therefore, use of a reference with different attenuation resulted in increased bias of AC estimates due to nonlinear distortion being this deviation larger when using low attenuating media.**

Index Terms— **Attenuation coefficient, spectral log difference, quantitative ultrasound, nonlinearity parameter**

I. Introduction

Ultrasonic attenuation has been explored in tissue characterization for decades including recent studies in liver [1], breast [2], placenta [3], or indirectly in muscle [4], among others biological tissues. Assuming linear acoustic propagation, the estimation of the attenuation coefficient (AC) in the frequency domain is straightforward because the power spectra of a gated backscattered signal can be modeled as a product of the system acquisition effects (i.e., scanner, transducer, beam) and effects derived from intrinsic acoustic properties of the medium (i.e., attenuation, backscatter coefficient). Several attenuation estimation methods in the frequency domain are outlined in [5].

However, acoustic propagation is a more complex phenomenon because every medium is inherently acoustically nonlinear. The Gol'dberg number can be used as a rule of thumb to predict the degree of acoustic nonlinearity in a medium. Assuming monochromatic plane wave propagation, the Gol'dberg number is computed as $\Gamma = \frac{\beta k M}{\alpha}$, where k is the wave number, $\beta = 1 + \frac{1}{2}\frac{B}{A}$, B/A is the acoustic nonlinearity parameter of the medium, M is the Mach-number equal to the particle velocity amplitude divided by the equilibrium speed of sound of the medium, and α is the attenuation coefficient. $\Gamma \ll 1$ means that acoustic nonlinearity might be negligible, whereas $\Gamma \gg 1$ means significant nonlinearitiy can be expected. Strong acoustic nonlinearity implies the generation of harmonics (2nd, 3rd, etc.) where energy is transferred out of the fundamental band.

Most attenuation estimation methods use the power spectra of the fundamental band. Therefore, we hypothesized that harmonic generation might lead to inaccuracies in attenuation estimation especially when large acoustic pressures are used. In the present work we analyzed a representative method for AC estimation in the frequency domain, namely, the spectral log difference for estimating the AC. Ultrasonic waveforms distorted by acoustic nonlinearity were obtained from computer simulations of nonlinear media; and using a high power pulse/receiver in experiments with physical phantoms.

II. Methods

A. Spectral-log-difference

The attenuation coefficient $\alpha(f)$ of a region of interest (ROI) having uniform scattering can be determined by computing the logarithm of the ratio of power spectra corresponding to two sub-windows, $S(f, z_p)$ and $S(f, z_d)$, from a proximal window and distal window, within the ROI, as

A. Coila and M. L. Oelze are with the Beckman Institute for Advanced Science and Technology, Department of Electrical and Computer Engineering, University of Illinois at Urbana-Champaign, IL, 61801, USA. e-mail: acoila@illinois.edu.

$$\log \frac{S(f,z_p)}{S(f,z_d)} = \log \frac{D(f,z_p)}{D(f,z_d)} + 4\alpha(f)(z_d - z_p) \quad (1)$$

where

$$S(f,z_p) = P(f)D(f,z_p)b(f,z_p)A(f,z_0)e^{-4\alpha(f)(z_p - z_0)},$$
$$S(f,z_d) = P(f)D(f,z_d)b(f,z_d)A(f,z_0)e^{-4\alpha(f)(z_d - z_0)},$$

$D(f,z_p)$ and $D(f,z_d)$ correct for the beam diffraction for the power spectra of the proximal and distal windows, respectively. Moreover, additional data acquisition is obtained from a well characterized reference phantom using the same settings such that

$$\log \frac{S_R(f,z_p)}{S_R(f,z_d)} = \log \frac{D_R(f,z_p)}{D_R(f,z_d)} + 4\alpha_R(f)(z_d - z_p), \quad (2)$$

where the subscript *R* stands for reference. If the speed of sound is approximately the same for the unknown medium and the reference phantom, the diffraction terms can be eliminated. Therefore, the attenuation coefficient can be computed as

$$\alpha(f) = \frac{1}{4L}\left[\log \frac{S(f,z_p)}{S_R(f,z_p)} - \log \frac{S(f,z_d)}{S_R(f,z_d)}\right] + \alpha_R(f) \quad (3)$$

where $L = z_d - z_p$. The attenuation coefficient slope (ACS) is the slope of the $\alpha(f)$ vs. f, where f corresponds to frequencies in the analysis bandwidth corresponding to the fundamental band.

B. Computer simulation

Computer simulated data were generated with the k-Wave MATLAB toolbox [6]. Three random media X, Y, and Z (2% standard deviation impedance) with same acoustic nonlinearity parameters (6.6) but different ACSs: 0.6, 0.9, and 0.2 dB/cm/MHz, respectively, were simulated. The source (and sensor) had a diameter of 0.5" and a 1" focal length and were configured in a 3-dimensional (3D) grid with 8.8 MHz maximum supported frequency (this limitation was set by the available computational resources). Then, a 30% bandwidth, Gaussian modulated pulse of 3.5 MHz center frequency was used at the source so that the second harmonic frequency was within the supported frequency range of the 3D grid. Echoes received at the sensor were recorded for four source pressures: 100 kPa, 500 kPa, 1MPa, and 1.5 MPa to assess different scenarios of acoustic nonlinear development. One hundred realizations for each media were simulated in order to smooth out the power spectra for the spectral log difference method.

The AC of medium X was determined using the spectral log difference method in two cases: (1) medium Y (more attenuating) as reference phantom and (2) medium Z (less attenuating) as reference phantom. The -6-dB bandwidth of the power spectra was used as the analysis bandwidth for estimation of the ACs.

C. Experimental phantoms

For the physical experiments, three tissue-mimicking phantoms, labelled A, B and C having estimated ACS values of 0.6, 0.9, and 0.2 dB/cm/MHz, respectively, and B/A $\approx$ 6.6 for each phantom [7] were scanned using a single-element spherically focused transducer (f/2) having a 0.5" diameter and 5-MHz nominal frequency (ISR054, NdtXducer LLC, USA). The phantoms were scanned using six excitation levels (see Table I) from a high-power pulsing apparatus (RAM-5000, Ritec, USA). The input signal applied to the transducer was a 1-cycle sinusoidal at 5-MHz.

The AC of the phantom A was determined using the spectral log difference method in two cases: (1) phantom B as reference phantom and (2) phantom C as reference phantom. The analysis bandwidths for estimation of the ACs was chosen following the same -6-dB criterion as in the simulation part.

TABLE I: Summary of peak positive pressure and peak negative pressure values associated with the settings used in the experiments, measured using a needle hydrophone at the focus of the transducer.

	Peak positive pressure (MPa)	Peak negative pressure (MPa)
Excitation level 1	7.58	2.78
Excitation level 2	9.10	3.38
Excitation level 3	10.22	3.83
Excitation level 4	11.02	4.21
Excitation level 5	11.54	4.52
Excitation level 6	12.10	4.74

III. Results

A. Computer simulation

Figure 1(a) shows the normalized averaged power spectra of backscattered echoes for media X (sample) and Y (reference) from the gated proximal and distal windows (20 λ axial length) centered at 12 and 24 mm depth, respectively. For the transducer geometry used in the computer simulation, the Rayleigh gain was $\frac{\pi a^2}{\lambda} \approx 11.6$. Therefore, the maximum Gol'dberg numbers considering peak pressures at the focal length were between $\Gamma_X \in [1.35, 20]$, $\Gamma_Y \in [0.9, 13.5]$, and $\Gamma_Z \in [4, 61]$, over the source pressures range. Therefore, a strong second harmonic (centered around 7 MHz) was observed when using the largest source pressure. Similar behavior was observed for media X (sample) and Z (reference) Fig. 1(b) shows the strongest 2nd harmonic development for the lower attenuating medium Z as expected from the Gol'dberg number calculation.

The attenuation coefficient estimate of medium X using the references Y (high attenuating) and Z (low attenuating) are shown in Fig. 2(a) and 2(b), respectively. We used an

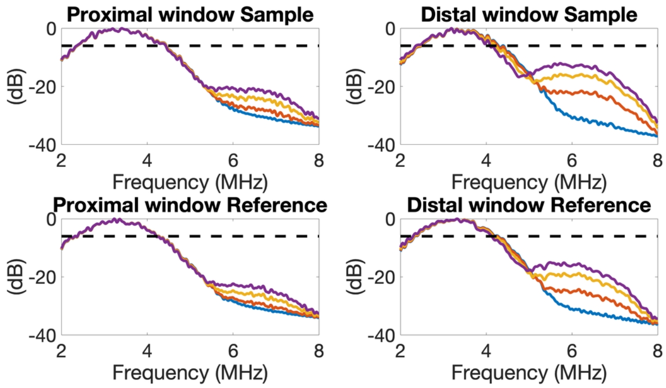

(a) Sample X (B/A = 6.6 and ACS = 0.6 dB/cm/MHz). Reference Y (B/A = 6.6 and ACS = 0.9 dB/cm/MHz)

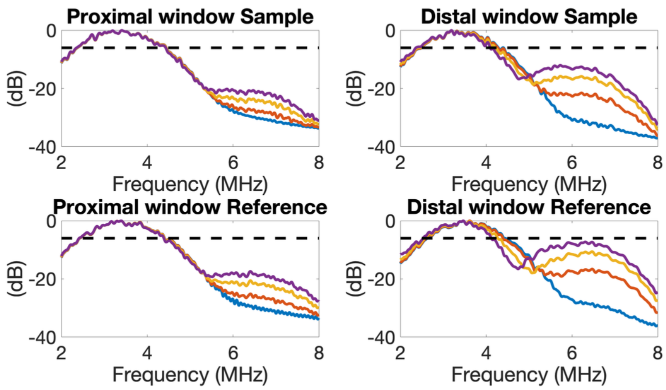

(b) Sample X (B/A = 6.6 and ACS = 0.6 dB/cm/MHz). Reference Z (B/A = 6.6 and ACS = 0.2 dB/cm/MHz)

Fig. 1: Top. Power spectra from gated proximal and distal windows, respectively, using 100 kPa (blue), 200 kPa (orange), 1 MPa (yellow) and 1.5 MPa (purple) source pressures (-6-dB level in dashed). Second harmonic is stronger in the distal window located in focal region. Higher second harmonic levels are produced at the largest source pressure 1.5 MPa. Both computer phantoms were simulated with the same nonlinearity parameter B/A. Hence, the stronger level of nonlinearity observed in the power spectra of the sample is due to the lower attenuation (0.6 dB/cm/MHz) compared with the reference (0.9 dB/cm/MHz). The low attenuating phantom is more sensitive to larger acoustic pressures. Bottom. Reference attenuation was lower (0.2 dB/cm/MHz) than that in the sample; hence, the stronger level of nonlinearity observed in the power spectra of the reference, although being simulated with the same B/A.

analysis bandwidth from 2.4 to 4.2 MHz (roughly 50% bandwidth). At low source pressures, the estimated ACS were consistent but for the highest pressure the ACS was +20% larger with a tendency to increase. When using the reference Z, however, the trend of the ACS decreased with larger source pressures decreasing by -20% and -40% at 1 MPa and 1.5 MPa source pressures, respectively. Thus, the deviation was strongly pronounced when the low attenuating phantom was used as reference.

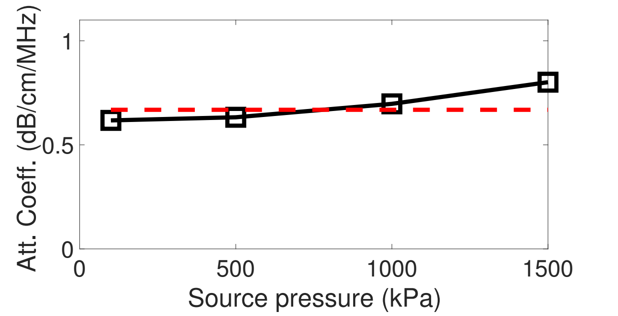

(a) Medium X - reference Y

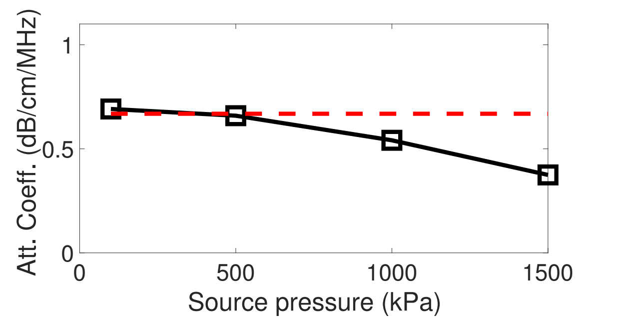

(b) Medium X - reference Z

Fig. 2: Attenuation coefficient slope of medium X, when using medium Y (top) and Z (bottom) as the reference. The ground truth attenuation coefficient set in simulations is depicted in dashed. The medium Z is low attenuating, hence, more sensitive to acoustic nonlinear effects.

B. *Experimental phantoms*

The AC estimates of phantom A using the references B (high attenuating) and C (low attenuating) are shown in Figures 3(a) and 3(b), respectively. It was observed that more consistent AC estimates were obtained when using references with higher attenuation coefficients, i.e., phantoms A and B, whereas more inconsistency was observed when using phantom C as the reference. Similar to the simulations, in this case, the Gol'dberg numbers for the phantoms A, B and C were in the range $\Gamma_A \in [8.8, 14]$, $\Gamma_B \in [5.9, 9.4]$, and $\Gamma_C \in [26.4, 42.1]$, respectively. Therefore, more nonlinear distortion of the fundamental band was expected in the phantom C, leading to more bias in AC estimates.

IV. Discussion

The presence of nonlinear distortion can be quantified through the Gol'dberg number, which is proportional to the ratio of the nonlinearity coefficient and attenuation. In computer simulations we confirmed that both the nonlinearity

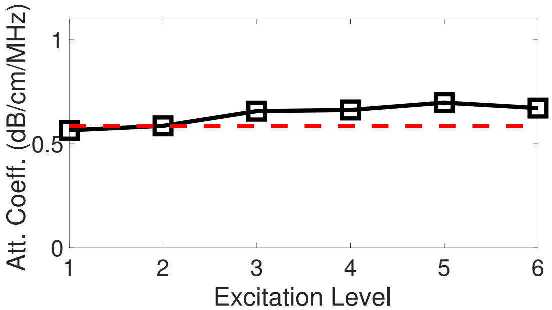

(a) Phantom A - reference phantom B

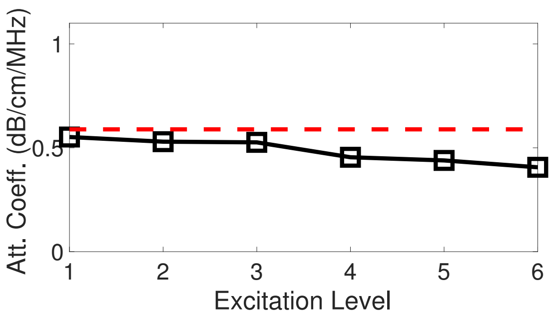

(b) Phantom A - reference phantom C

Fig. 3: ACS of phantom A, when using phantom B (top) and C (bottom) as the references. The ground truth AC using a through transmission technique is depicted in dashed. The phantom C had lower attenuation and, hence, was more sensitive to acoustic nonlinear effects.

parameter and the acoustic attenuation of the medium affect the generation of the 2nd harmonic. Thus, spectral methods for AC estimation that use the fundamental band might provide biased AC estimates when non negligible energy is transferred out of the fundamental band.

In the physical experiments, we hypothesized that because the B/A values were approximately the same for each phantom, the effects of nonlinear distortion would be more pronounced in phantom C, which had much lower attenuation. Specifically, increased excess attenuation due to transfer of energy from the fundamental to the harmonics would be observed more in phantom C. Figure 3(a) shows the AC slope estimated for phantom A versus excitation level when using phantom B as a reference. The ACS estimate varied from 0.57 dB/cm/MHz at level one to 0.67 dB/cm/MHz at the level six, increasing quasi-monotonically. In contrast, when using phantom C as reference (Fig. 3(b)) the estimated ACS of phantom A decreased monotonically from 0.57 to 0.43 dB/cm/MHz as the excitation levels increased from level one to six. In the experiment, using references with different attenuation coefficients as the sample resulted in increased bias of AC estimates due to nonlinear distortion. This is because higher frequencies are more rapidly transferred to higher harmonics resulting in a sloping effect over distance in the backscattered power spectra for lower attenuating media. When using a more attenuating reference phantom, and assuming low nonlinear distortion at the proximal window, the slope of the distal window in the sample is more attenuated than in the reference. Thus, by the negative sign in Eq. 3, an apparent increase in ACS can explained. The opposite (decreasing ACs over excitation levels) occurs when the reference phantom has lower attenuation than the sample. However, the effect is strong because the nonlinear effects are enhanced in low attenuating media.

In conclusion, the study findings suggest that the ACS estimates can be biased when large acoustic pressures are employed in the spectral log difference method. To prevent biases, tradeoffs between the attenuation of the reference material, B/A and needs for signal strength should be considered.

ACKNOWLEDGMENT

A. Coila acknowledges the financial support from the National Council of Science, Technology and Technological Innovation (CONCYTEC, Perú) through the National Fund for Scientific, Technological Development and Technological Innovation (FONDECYT, Perú) under grant 132-2016. The authors also acknowledge grants from the NIH (R21EB024133 and R21EB023403).

REFERENCES

[1] S. K. Jeon, J. M. Lee, I. Joo, J. H. Yoon, D. H. Lee, J. Y. Lee, and J. K. Han, "Prospective evaluation of hepatic steatosis using ultrasound attenuation imaging in patients with chronic liver disease with magnetic resonance imaging proton density fat fraction as the reference standard," *Ultrasound Med. Biol.*, vol. 45, no. 6, pp. 1407–1416, 2019.

[2] H. G. Nasief, I. M. Rosado-Mendez, J. A. Zagzebski, and T. J. Hall, "A quantitative ultrasound-based multi-parameter classifier for breast masses," *Ultrasound Med. Biol.*, vol. 45, no. 7, pp. 1603 – 1616, 2019.

[3] F. Deeba, M. Ma, M. Pesteie, J. Terry, D. Pugash, J. A. Hutcheon, C. Mayer, S. Salcudean, and R. Rohling, "Attenuation coefficient estimation of normal placentas," *Ultrasound Med. Biol.*, vol. 45, no. 5, pp. 1081 – 1093, 2019.

[4] W. C. Weng, C. W. Lin, H. C. Shen, C. C. Chang, and P. H. Tsui, "Instantaneous frequency as a new approach for evaluating the clinical severity of duchenne muscular dystrophy through ultrasound imaging," *Ultrasonics*, vol. 94, pp. 235 – 241, 2019.

[5] Y. Labyed and T. A. Bigelow, "A theoretical comparison of attenuation measurement techniques from backscattered ultrasound echoes," *J. Acoust. Soc. Am.*, vol. 129, no. 4, pp. 2316–2324, 2011.

[6] B. E. Treeby, J. Jaros, A. P. Rendell, and B. T. Cox, "Modeling nonlinear ultrasound propagation in heterogeneous media with power law absorption using a k-space pseudospectral method," *J. Acoust. Soc. Am.*, vol. 131, no. 6, pp. 4324–4336, 2012.

[7] F. Dong, E. L. Madsen, M. C. MacDonald, and J. A. Zagzebski, "Nonlinearity parameter for tissue-mimicking materials," *Ultrasound Med. Biol.*, vol. 25, no. 5, pp. 831–838, 1999.